



ELSEVIER

Journal of Chromatography A, 908 (2001) 185–200

JOURNAL OF
CHROMATOGRAPHY A

www.elsevier.com/locate/chroma

Modification of a commercial chiral stationary phase Influences on enantiomer separations using simulated moving bed chromatography

E. Huthmann, M. Juza*

CarboGen Laboratories (Aarau)^{AG}, Schachenallee 29, CH-5001 Aarau, Switzerland

Abstract

Chromatographic enantiomer separations using high-performance chromatography and the simulated moving bed (SMB) principle have become a practically useful method for obtaining optical isomers. The carbamate derivatives of amylose coated onto silica particles are very effective chiral stationary phases (CSPs). Several lots of Chiralpak[®] AS[™], and its successor, Chiralpak[®] AS-V[™], were compared by laser diffraction, microscopic imaging and pulse injections with increasing amounts of various racemates in order to determine the loading capacity and the competitive adsorption isotherms. Software simulations allowed to assess the possible effects due to the observed variations between the CSPs on the performance of a pilot SMB unit. The obtained results were verified by two multi-kilogram separations performed under current good manufacturing principles (cGMP) guidelines employing the two CSPs. The results of the two production runs are discussed in the light of the recently introduced “triangle theory” which allows to account for the overload conditions prevailing under preparative chromatographic conditions and to predict optimal operating conditions. Under optimized conditions the enantiomer separation of 1.4 kg racemate/kg stationary phase per day with purities >99.6% for the target enantiomer have been achieved. © 2001 Elsevier Science B.V. All rights reserved.

Keywords: Chiral stationary phases, LC; Enantiomer separation; Simulated moving bed chromatography; Preparative chromatography; Tröger's base

1. Introduction

Simulated moving bed (SMB) chromatography on chiral stationary phases (CSPs) has become an essential tool for the chromatographic resolution of racemates on a preparative scale and provides an important alternative to enantioselective synthesis and chemical resolutions [1]. Compared to conventional batch chromatography, SMB chromatography

has the benefits of a continuous process which affords a constant product purity without permanent control of all collected fractions. Less solvent is used as for a batch separation [2]. This advantage results from the overload conditions under which the columns of such units are usually operated in order to exploit the loading capacity of the CSP. Under these conditions the retention behavior of the enantiomers to be separated becomes dependent on their concentration in the stationary phase and has to be described by “competitive adsorption isotherms”. During the last years criteria for the optimal design

*Corresponding author.

E-mail address: markusjuza@carbogen.com (M. Juza).

of SMB systems have been developed, which allow to account for the nonlinear character of the involved adsorption equilibria and to optimize the productivity per kg CSP easily [3]. Following the so-called “triangle theory” constraints on these criteria can be derived which allow for complete separation of a binary mixture following the Langmuir and the modified Langmuir isotherm [4] and the most general case of a bi-Langmuir multicomponent adsorption isotherm [5].

Among the commercially available CSPs especially the polysaccharide derivatives have proven their great versatility for enantiomer separations in analytical chromatography [6,7] and for preparative separations using batch chromatography [8] and SMB [9,10]. During the recent years amylose carbamates coated on silica particles have gained increasing importance for the separation of racemates not resolved on microcrystalline cellulose triacetate [11], cellulose tribenzoate [12] or cellulose carbamates [13]. These amylose-derived CSPs allow the separation of amounts typically ranging from 0.2 to 2 kg racemate/kg CSP per day [14,15] through SMB chromatography. For industrial applications in the pharmaceutical field very narrow specifications for the CSPs and the products separated on them have to be met and the consequences of non-satisfactory separations or production delays can have considerable impact on the registration process and the time to market for an API (active pharmaceutical ingredient).

Thus the recent modification in the production process of the CSP Chiralpak® AS™ (now marketed in Europe under the name Chiralpak® AS-V™) made it inevitable to study the properties of this stationary phase in detail and to compare its properties with previous production lots of this CSP.

2. Experimental

2.1. Analytical chromatography

Analysis of the product streams and overload measurements were carried out on four 250×4.6 mm I.D. columns, containing Chiralpak® AS™ and Chiralpak® AS-V™ with a pore size of 1500 Å and a

nominal particle size of 20 µm. Columns 1 and 2 were packed with Chiralpak® AS™ material provided by Chiral Technologies, Strassbourg, France by Grom (Herrenberg, Germany); columns 3 and 4 were obtained from Chiral Technologies, Strassbourg, France. All columns had a bed porosity of $\epsilon^*=0.4$. Injection loop volume and extra-column dead volume were 250 µl and 220 µl, respectively. The mobile phase consisted of *n*-hexane–isopropanol (99:1; v:v, both HPLC grade, J.T. Baker, Deventer, Netherlands) for the separation of *trans*-stilbene oxide (Aldrich, Buchs, Switzerland) and acetonitrile (HPLC grade, J.T. Baker) for the separation of Tröger’s Base (Aldrich) and compound A (synthesized in GarboGen’s laboratories) at a flow-rate of 1.00 ml/min. The operating temperature was 30°C for all measurements. All chromatograms were measured on an HP 1090 system (Hewlett-Packard, Basel, Switzerland) equipped with an 6 mm flow cell and connected to a Kajak XA HP Chemstation (Hewlett-Packard). The UV diode array detection (DAD) system was operated simultaneously at 234, 254, 280 and 330 nm.

2.2. SMB separation

Compound A, synthesized under cGMP guidelines in our laboratories, was separated employing pure acetonitrile (Schweizerhall, Basel, Switzerland) as eluent (cf. Section 4.4). The bulk stationary phases were Chiralpak® AS™ and Chiralpak® AS-V™ (20 µm) purchased from Chiral Technologies. Analytical assay of extract and raffinate stream was performed without dilution employing the same stationary phase and eluent as for the preparative separation.

2.3. Column packing and testing

Bulk Chiralpak® AS™ and Chiralpak® AS-V™ were packed into eight NW-50 columns purchased from Merck (Darmstadt, Germany). The bedlength of the eight columns used ranged from 107 to 114 mm; the I.D. of the columns was 48 mm. Each column contained exactly 110.00 g dry mass of the stationary phase and gave an averaged bed length of about 107 mm. All columns were tested with a preparative HPLC system provided by Knauer (Berlin, Germany), which consisted out of a K-1800

pump with a 1000 ml/min pump head, a HPLC-Box and an K-2500 UV detector. In the case of Chiralpak® AS™, the retention times for compound A, measured at an flow-rate of 50 ml/min, were (averaged over the eight columns) 3.074 ± 0.076 min SD and 3.590 ± 0.114 min SD; for Chiralpak® AS-V™, the retention times for compound A, measured at an flow-rate of 50 ml/min, were (averaged over the eight columns) 3.478 ± 0.029 min SD and 4.391 ± 0.096 min SD.

2.4. Determination of adsorption isotherms

Four analytical HPLC columns (cf. Section 2.1), containing various lots of Chiralpak® AS™ and Chiralpak® AS-V™, were installed into a HP 1090 system equipped with a Jasco CO1560 oven (Omnilab, Mettmenstetten, Switzerland) and thermostated at $30 \pm 0.1^\circ\text{C}$, the operating temperature of the SMB unit. Racemates of *trans*-stilbene oxide, Tröger's base and compound A were injected at increasing concentrations (cf. Tables 4–7). The obtained data was entered into the Novasep software (cf. Section 2.6) to determine the modified competitive Langmuir adsorption isotherms and SMB operating conditions.

2.5. SMB unit

A Licosep 10×50, produced by Novasep (Vandoeuvre les Nancy, France) was used for the experiments. A detailed description of the unit has been given recently [16]. It was equipped with eight NW-50 (non-jacketed) columns produced by Merck with a variable bed length ranging from 15 mm up to 119 mm and an inner diameter of 48 mm that can be self-packed easily. A schematic overview of the system components is given in Fig. 1.

2.6. SMB hard- and software

The Licosep 10×50 SMB unit from Novasep is controlled by a central system composed of a Siemens PLC (type S7-300) and a PC (P200, Siemens Nixdorf, Stuttgart, Germany) as the user interface. The supervision software works under

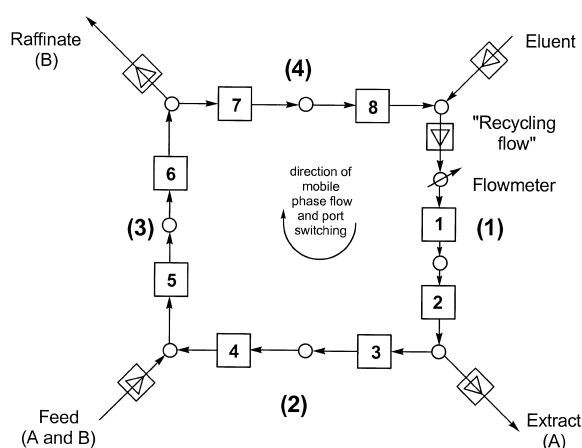


Fig. 1. Schematic flow diagram of the Licosep 10×50 unit with a 2-2-2-2 column configuration in the first period of a cycle. Flow direction and location of the five pumps are indicated by triangles.

DOS and allows the full control of the unit parameters (valves, pumps, flow-rates, pressures) when the unit is running or under test. All relevant parameters and data are continuously stored in files for quality control. The software allows an easy access to real time curves (flow-rates, temperature, pressure). All measurements are transmitted from the Licosep 10×50 through a control board, containing the PLC and all required interfaces and supplies. A simulation software called “softSMB” is supplied with the system. It works under Windows 95 and allows to find a competitive adsorption isotherm based on overload injections and to optimize the operating parameters before starting the unit itself.

2.7. Particle characterization

Particle sizes were determined with a Sympatec HELOS/KA laser diffractometer (Sympatec, Clausthal-Zellerfeld, Germany) after preparing a dispersion of the particles in isopropanol and ultrasonically for 30 s. The light microscopic images were taken with a Polyvar Met (Reichert-Jung, Basel, Switzerland) equipped with a CCD DXC-950P camera (Sony, Zurich, Switzerland) using the AxioVis software by Zeiss (Oberkochen, Germany). The images were obtained using the transmitted light in brightfield illumination.

3. Background

SMB units contain four discrete sections (cf. Fig. 1), each composed of at least one chromatographic column. The time between two shifts of the injection and collection points after a predefined period is called switch time, t^* . It must be understood that a column can appear in any of these Sections (1–4), depending on the time at which it is observed. The duration of t^* is determined by the flow-rate of the solid-phase Q_S and its volume V_S in a hypothetical true moving bed (TMB) unit:

$$t^* = \frac{V_S}{Q_S}. \quad (1)$$

The key to the successful operation of the simulated moving bed are the four internal volumetric flow-rates, Q_j , $j = 1, \dots, 4$, in these sections, which have to be controlled rigorously. The internal flow-rates are related to the four external fluid streams through simple mass balance relations:

$$Q_1 = Q_{\text{Eluent}} + Q_4 \quad (2)$$

$$Q_2 = Q_1 - Q_{\text{Ex}} \quad (3)$$

$$Q_3 = Q_2 + Q_{\text{Feed}} \quad (4)$$

$$Q_1 = Q_3 - Q_{\text{Ra}} \quad (5)$$

Whenever four of the flow-rates are given (one of them being an internal flow-rate), the other four are defined also. Together with the overall void fraction of the columns, ε^* , the switch time t^* and the single column volume V the internal flow-rates determine the so-called flow-rate ratios, m_j , which are defined as the ratio of the net fluid flow-rate over the solid-phase flow-rate in each of the four sections of the TMB unit. Exploiting the equivalence between SMB and TMB [17] one obtains:

$$\begin{aligned} m_j &= \frac{\text{net fluid flow-rate}}{\text{solid flow-rate}} \\ &= \frac{Q_j t^* - V \varepsilon^*}{V(1 - \varepsilon^*)} \quad (j = 1, \dots, 4) \end{aligned} \quad (6)$$

Based on these flow-rate ratios m_j , the experimental performances of SMBs can be properly designed, interpreted and compared following a recently pre-

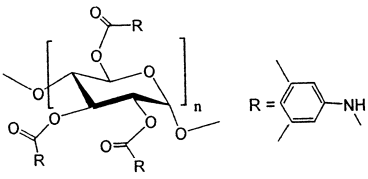
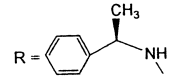
sented approach, which leads to criteria for the choice of optimal and robust operating conditions of such units [3]. It should be mentioned that already small changes in the internal flow-rates result in deviations from the optimal operating conditions (described by a set of four m_j , values and t^*) and cause impure extract and raffinate streams. Another *sine qua non* for optimal operation are minimized dead volumes and a set of very similar and stable chromatographic columns.

4. Results and discussion

Prerequisite for scaling up a chromatographic analytical chiral separation is that CSP is available in large amounts, with reproducible batch-to-batch properties and at a relatively low cost with respect to the value of the enantiomers to be separated. If this is fulfilled then the economical feasibility of a preparative separation or a SMB process will be dictated by the key properties of the CSP, namely selectivity, loading capacity and efficiency, which control the size of the unit and the achievable specific productivity of the process per unit mass of stationary phase. Beside these, other important issues are related to the behavior of CSP in time. These refer to its chemical stability, which limits the number of compatible mobile phases and indirectly the maximum solubility of the solute, its mechanical stability, which is particularly important in HPLC applications where small particle sizes are adopted and large pressure drops are imposed, and its lifetime. All these characteristics have to be properly taken into account when selecting the CSP for a specific chiral separation.

Natural products such as cellulose and amylose have proved to be of great versatility for enantiomer separation. Though poor chiral selectors in their native state, they become highly effective when their hydroxyl functions are derivatized, particularly with aromatic moieties through ester or carbamate linking [6,7] and they are properly immobilized on silica supports (cf. Table 1 for examples). These materials are composed of small chiral units regularly repeating along the polymeric chain; hence the density of active sites capable of chiral recognition is very high and results in a high loading capacity.

Table 1
The chiral stationary phases Chiralpak® AD™ and Chiralpak® AS™

Structure of CSP	Chiral selector	Compatible solvents ^a	Trade name
	Amylose tris(3,5-dimethylphenylcarbamate)	Hexane–ethanol (100:0–0:100)	Chiralpak® AD™
	Amylose tris[(S)-methylbenzylcarbamate]	Hexane–2-propanol (100:0–0:100)	Chiralpak® AS™ or AS-V™

^a Examples.

Table 1 lists the functional groups of two of the most used CSPs derived from amylose, together with compatible solvent mixtures. The tris(3,5-dimethylphenyl carbamate) derivative of amylose has been commercialized under the name Chiralpak® AD™, the tris[(S)-methylbenzylcarbamate] has been named Chiralpak® AS™. The latter derivative, as well as providing polar, polarizable sites, also contributes another chiral center to improve enantioselectivity. It should be noted that the (S)-configured methyl group provides a greater chiral recognition ability than the (R,S) and the (R)-derivative [18]. The chiral polymers are not attached to the support covalently, but rather are coated on silanized, wide-pore silica gel (cf. Fig. 2).

Consequently, chromatographers must exercise

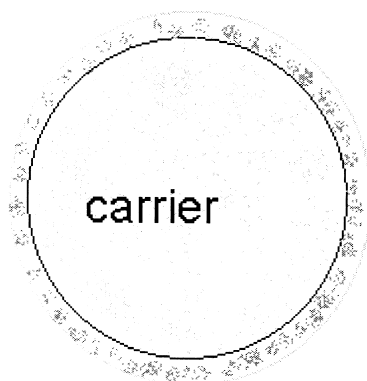


Fig. 2. Schematic representation of the chiral stationary phases coated on the spherical inorganic support, silica.

some caution when choosing chromatographic conditions (mobile phase solvents, pressure, temperature) for SMB or batch separations. These CSPs are most often used in the normal-phase mode (i.e. with solvents like hexane and ethanol). To prevent peak tailing small amounts of organic acids (trifluoroacetic acid, TFA) or bases (diethylamine (DEA), triethylamine (TEA)) can be used that may help to block any active sites and improve peak symmetry.

Chiralpak® AS™ is one of the newest members of the CSP family commercialized by Daicel, Japan, first described by Okamoto et al., ten years ago [19]. It has been used e.g. for the HPLC separation of methyl jasmonat [20] and amide conjugates of jasmonic acid [21], 1-azabicyclo [2.2.1]heptane-3-one and pyrrolidin derivatives [22], protected α -amino acids [23] and chiral selenoxides [24] and has been employed for supercritical fluid chromatography [25]. Also the semi-preparative purification of benzofuroxane derivatives [26] and the isolation of an API on a kg scale [8] have been described. The mechanisms governing the chiral discrimination have been studied in detail by Roussel and co-workers [27,28].

An example for changes in retention behavior depending on the manufacturing process of the CSP is the separation of Tröger's base on Chiralpak® AS™ and the recently introduced successor of that phase, Chiralpak® AS-V™. As can be seen in Fig. 5, the two enantiomers of Tröger's base are not baseline resolved (cf. Fig. 3, top; $\alpha = 1.17$; $R_s = 0.973$) on Chiralpak® AS™, whereas on

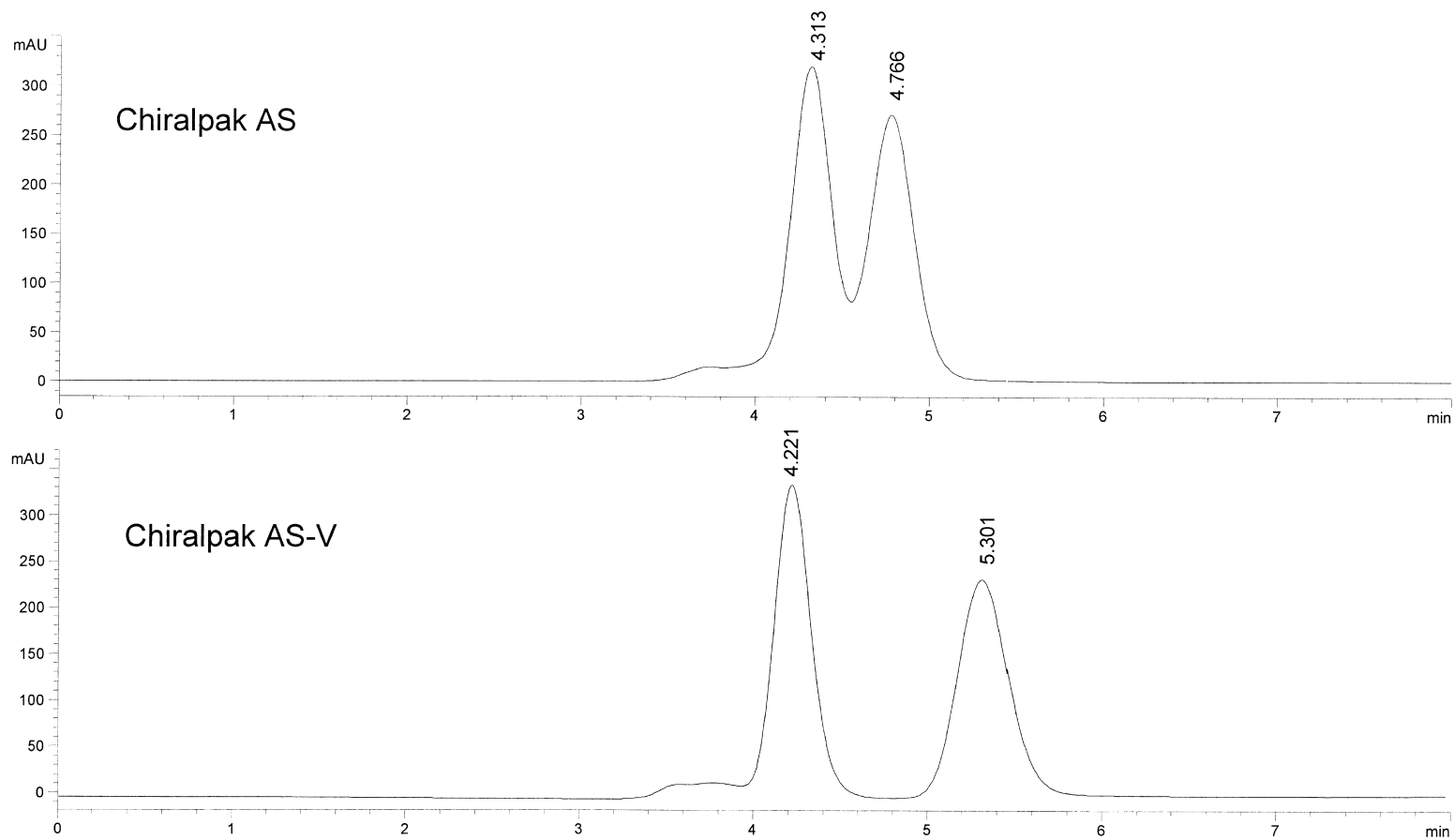


Fig. 3. Separation of Troger's base on Chiralpak[®] AS[™], column dimensions: 250×4.6 mm I.D.; $T=30^{\circ}\text{C}$, particle size: 20 μm , eluent: acetonitrile, detection: 254 nm, flow-rate: 1.00 ml/min; top: Chiralpak[®] AS[™], bottom: Chiralpak[®] AS-V[™].

Chiralpak® AS-V™ (cf. Fig. 3, bottom; $\alpha=1.42$; $R_s=2.193$) an excellent separation can be obtained.

These results prompted us to characterize some of the batches of this CSPs used in our laboratories in more detail, giving special regard to the increasing back pressure observed during the separation of compound A on Chiralpak® AS™ and the modified retention behavior due to the new production process for the AS phase.

4.1. Characterization of chiral stationary phases

The majority of currently used preparative CSPs are coated on spherical silica particles. They are easier to pack and show high-performance, good column stability and lower back pressure than irregular packings. For preparative or SMB chromatography particle size and particle size distribution are of special interest since the pressure drop is proportional to the bed length divided by the particle size squared. Only a very narrow distribution of particle sizes will give reproducible results in the up-scaling process of a separation from analytical HPLC to SMB. In Table 2 some of the physical properties of the two Chiralpak® AS™ phases [29] are summarized.

The differences between the two CSPs are rather small and will not explain e.g. the variations in the enantioselectivity of Tröger's base (cf. Fig. 3) or any increased back-pressure when working with Chiralpak® AS™.

In order to obtain some insight on the size distribution of the particles we had the bulk stationary phases analyzed for particle sizes by the Fraunhofer diffraction method [30] (cf. Fig. 4). As can be seen the particle sizes distribute over a very narrow

range, with a nearly Gaussian distribution centered around 24 μm . No significant differences between the two CSPs can be observed, however, the curve for Chiralpak® AS™ (cf. Fig. 4 top) shows a distinct shoulder (arrow in Fig. 4), thus indicating the presence of a non-negligible amount of larger particles and/or agglomerates of two and more particles. Such agglomerates must result from the coating procedure of the CSP, connecting two or more particles (cf. Fig. 2) through a bridge of the coating, since they could not be destroyed by ultrasonating the samples dispersed in *n*-hexane or isopropanol (cf. Section 2.7).

The S-shaped curve overlaid to the particle size distribution curves give an indication of the summed-up amounts of particles found between the starting point of the measurements (0.9 μm) and the end (175 μm). The particle sizes between 1 and 10 μm only add a small portion to the distribution as do the particle sizes over 65 μm . The measurements indicate that more than 80% of all particles have a size between 15 and 34 μm (cf. Table 3).

The distribution of the particle sizes does not change after use (cf. Section 4.4) within the experimental error of the measurements, thus indicating that the material is stable over a longer time and no breakdown of the spherical particles takes place. These results were corroborated by (light) microscopic images [31] taken before and after use of the Chiralpak® AS™ and Chiralpak® AS-V™ (cf. Fig. 5).

The single particles can easily be distinguished as black dots and their spherical appearance is obvious. However, compared to Chiralpak® AS-V™ (Fig. 5c and d) for Chiralpak® AS™ a wider distribution of particle sizes can be seen (cf. Fig. 5a and b). Several

Table 2
Properties of Chiralpak® AS™ and Chiralpak® AS-V™

Trade name	Lot No.	Particle size d50 ^a (μm)	Particle size d10 ^b (μm)	Pore size (μm)	Carbon content (%)	Loss on drying (%)
Chiralpak® AS™	ASOOSC-HB001	28.6	20.4	0.155±0.4	12.8	0.3
Chiralpak® AS-V™	T300AS-V00SC- IK002	28.3	20.4	n.g. ^c	n.g. ^c	0.6

^a Average particle size.

^b Diameter at which 10% of the particles are smaller.

^c Not given.

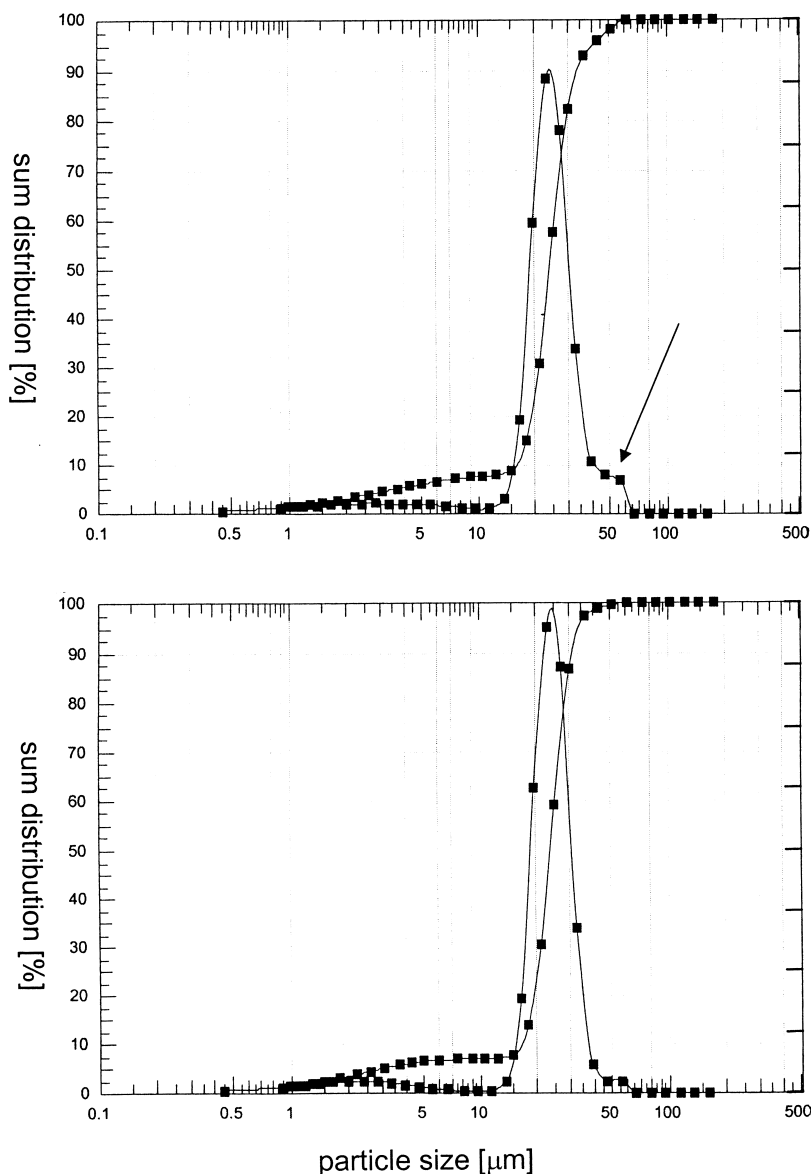


Fig. 4. Particle size distribution of Chiralpak[®] AS[™] and Chiralpak[®] AS-V[™] determined by laser diffraction.

small particles and conglomerates of particles adhering to one another can be observed (indicated by arrows). This effect is less pronounced with the new type of CSP, Chiralpak[®] AS-V[™] before (cf. Fig. 5c) and after use (cf. Fig. 5d).

Even though some physical differences between the two types of CSP can be seen, they do not account for the chemical diversity, i.e., the variations

in the formation of the diastereomeric association complexes needed for chiral discrimination as seen e.g. in Fig. 3. However, the presence of agglomerated particles (cf. Fig. 5b) could explain the increasing back-pressure during the separation of compound A on Chiralpak[®] AS[™]. The operation of the SMB causes the internal flow-rates to change frequently with t^* (cf. Section 3) and gives rise to a mechanical

Table 3
Particle sizes and their distribution for Chiralpak® AS™ and Chiralpak® AS-V™

CSP		Median value ^a (μm)	d10 ^b (μm)	d90 ^c (μm)
Chiralpak® AS™	Before use	23.9	15.7	34.7
	After use	24.0	15.9	34.1
Chiralpak® AS-V™	Before use	23.8	16.3	32.1
	After use	23.7	16.3	32.4

^a Average particle size.

^b Diameter at which 10% of the particles are smaller.

^c Diameter at which 10% of the particles are bigger.

stress on the particles. Whenever agglomerates break apart, small parts of the coating and silica will be released which eventually follow the mobile phase flow (~300 ml/min, equivalent to ~4300 l/day) and will be trapped in the frits of the columns. These particles will block a part of the frit and thus cause an increased back-pressure.

4.2. Determination of competitive adsorption isotherms

In order to establish differences in the retention behavior of the two types of CSP under investigation and their concentration dependent adsorption properties two test substances, Tröger's base and *trans*-stilbene oxide, and a racemate synthesized in our laboratories (compound A, structure cannot be disclosed due to proprietary reasons) were injected in analytical amounts on four HPLC columns containing Chiralpak® AS™ and AS-V™ (cf. Tables 4–6 and Section 2.1).

Tables 4–6 give an overview of the analytical pulse injections performed on the five different columns. Columns 1 and 2 were packed by a contract laboratory with bulk Chiralpak® AS™ material, columns 3 and 4 were obtained directly from the manufacturer of the CSP and contained Chiralpak® AS™ and AS-V™, respectively. Quite

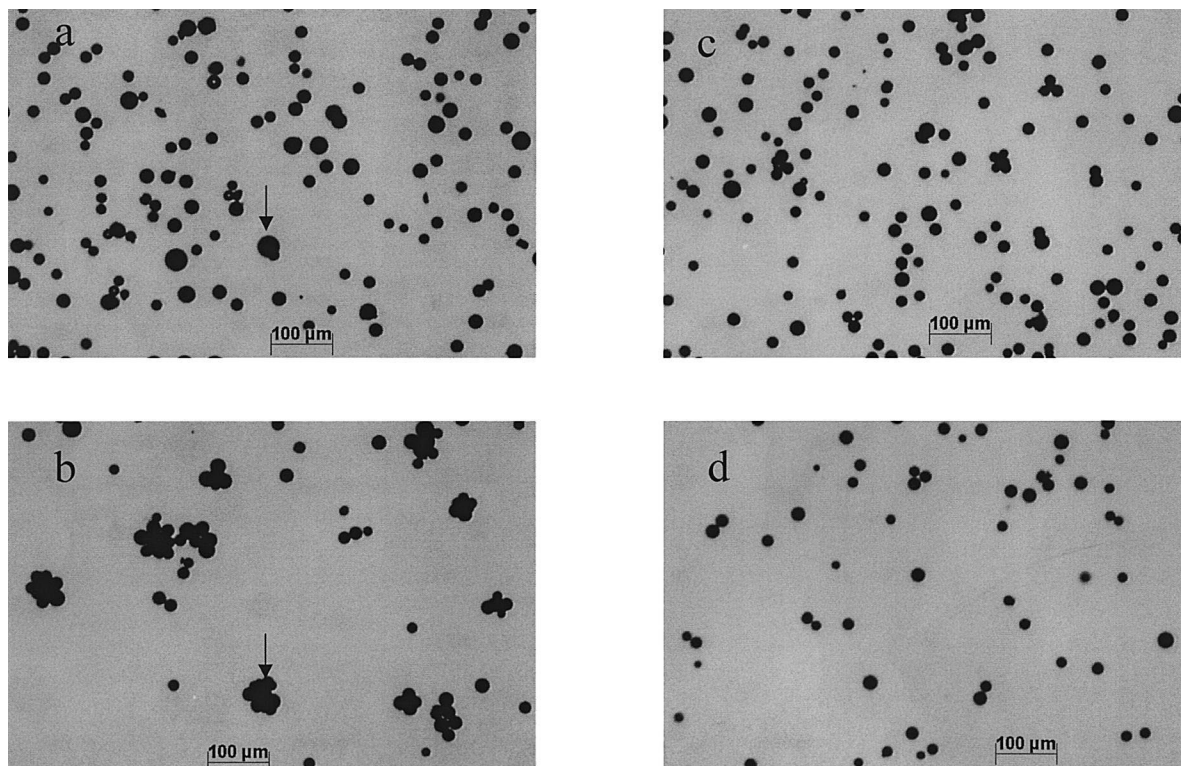


Fig. 5. Microscopic images of Chiralpak® AS™ (a and b) and Chiralpak® AS-V™ (c and d) before and after use, respectively, enlargement given in the pictures.

Table 4
Separation of Tröger's base on Chiralpak® AS™ columns^a

Column No.	CSP	t_{R1}	t_{R2}	α	R_s
1	AS	3.493	3.835	1.18	0.63
2	AS	3.538	3.972	1.23	0.72
3	AS	3.604	4.03	1.21	0.84
4	AS-V	3.59	4.45	1.44	1.74

^a Column dimensions: 250×4.6 mm I.D.; $T=30^\circ\text{C}$, particle size: 20 μm , eluent: acetonitrile, detection: 250 nm, flow-rate: 1.00 ml/min.

Table 5
Separation of *trans*-stilbene oxide on Chiralpak® AS™ columns^a

Column No.	CSP	t_{R1}	t_{R2}	α	R_s
1	AS	4.632	5.402	1.25	1.04
2	AS	4.187	4.574	1.156	0.67
3	AS	4.313	4.766	1.17	0.97
4	AS-V	4.221	5.301	1.42	2.19

^a Column dimensions: 250×4.6 mm I.D.; $T=30^\circ\text{C}$, particle size: 20 μm , eluent: acetonitrile, detection: 250 nm, flow-rate: 1.00 ml/min.

Table 6
Separation of compound A on Chiralpak® AS™ columns^a

Column No.	CSP	t_{R1}	t_{R2}	α	R_s
1	AS	6.053	6.697	1.14	0.91
2	AS	6.224	6.672	1.09	0.64
3	AS	4.819	5.094	1.08	0.57
4	AS-V	5.079	5.973	1.26	1.60

^a Column dimensions: 250×4.6 mm I.D.; $T=30^\circ\text{C}$, particle size: 20 μm , eluent: *n*-hexane–isopropanol (99:1, v/v) detection: 250 nm, flow-rate: 1.00 ml/min.

Table 7
Retention times of analytical and overloaded injections^a

Experiment No.	Concentration (g/l)	Injected volume (μl)	t_{R1} (min)	t_{R2} (min)
1	analytical	10	3.590	4.450
2	0.5	10	3.583	4.448
3	1.0	10	3.580	4.440
4	5.0	10	3.578	4.433
5	10.0	10	3.576	4.427
6	20.0	10	3.573	4.421
7	30.0	10	3.572	4.416
8	30.0	50	3.570	4.410
9	30.0	100	3.565	4.405

^a Flow rate: 1.00 ml/min; $T=30^\circ\text{C}$; detection at 254 nm.

surprisingly, the differences between the various columns are very pronounced, reaching from baseline separation for all three compounds to almost no separation. The compound least affected by the properties of the various lots of the CSP is *trans*-stilbene oxide which was resolved by using a small amount of isopropanol (1%, v/v) added to *n*-hexane as eluent. Tröger's base and compound A were resolved using pure acetonitrile as eluent (*trans*-stilbene oxide could not be separated using pure acetonitrile). Columns 1 and 2 show a considerable fronting of the peaks, probably due to a not successful packing procedure. However, the enantioselectivity for *trans*-stilbene oxide and Tröger's base is reasonably well. Column 2 shows good enantioselectivity for compound A and Tröger's base, but not for *trans*-stilbene oxide. Column 4 excels all other four columns dramatically, all three compounds are baseline-resolved and the eluted enantiomers show symmetrical peak shapes.

Summarizing, the best resolution and chromatographic behavior for all compounds could be obtained on the column packed with Chiralpak® AS-V™.

Among the most important mechanisms governing preparative and simulated moving bed chromatographic applications is the thermodynamic equilibrium of the separation system under overloaded conditions. Therefore increasing amounts and volumes of the three racemates were injected on the four columns containing Chiralpak® AS™ and AS-V™ and the resulting retention times were measured. As an example the data obtained for the resolution of compound A on column 4 are shown in Table 7 and Fig. 6.

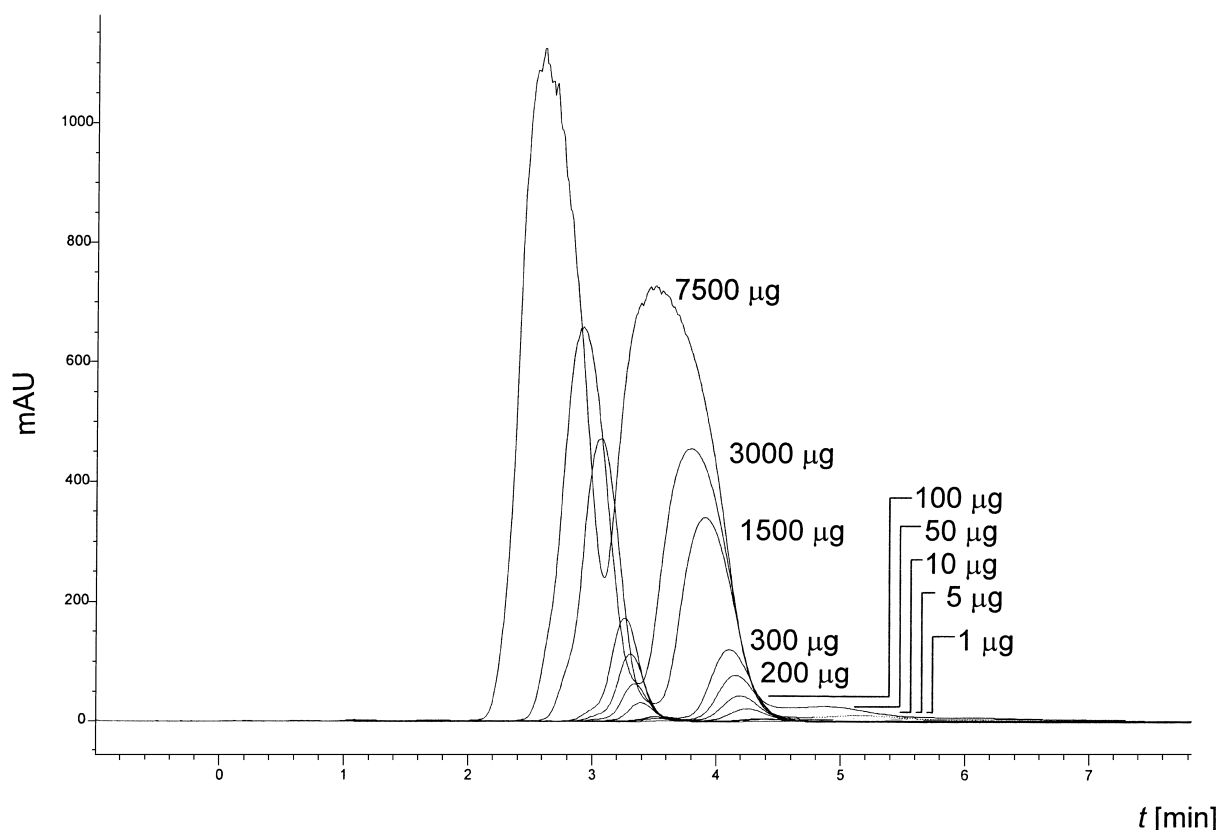


Fig. 6. Overload injections of compound A on Chiralpak[®] AS-V[™]; column 5: 250 mm×4.6 mm I.D., 20 µm; mobile phase: acetonitrile; detection: 254 nm; $T=30^{\circ}\text{C}$.

Based on pulse injections on the four HPLC columns filled with Chiralpak[®] AS[™] and Chiralpak[®] AS-V[™] with increasing amounts of the three racemates (cf. e.g. Fig. 6 and Table 7) the Novasep software package “softSMB” allows to correlate through a curve-fitting procedure the equilibrium experimental results with a postulated modified Langmuir competitive isotherm which takes the form:

$$n_i = \lambda \cdot c_i + \frac{\bar{N}_i K_i c_i}{1 + \sum_{k=1}^2 K_k \cdot c_j} \quad (7)$$

In this equation n_i and c_i are the adsorbed and the fluid phase concentration, respectively; λ is a dimensionless coefficient; K_i is the equilibrium constant of the i th component, which accounts for the overload effects; the upper limit of n_i is given by the saturation capacity \bar{N}_i .

This isotherm is often applied to the modeling of competitive adsorption behavior of racemic mixtures taking into account the adsorption on a heterogeneous surface (cf. Fig. 2) that consists of two different types of adsorption sites, e.g. a non-chiral interaction (linear term) and an enantioselective discrimination site with different affinity for the two chiral substances (Langmuirian term). The assumption that the non-chiral adsorption sites cannot be saturated is true only for low concentrations, at high concentrations their adsorption behavior will also become dependent on the mobile phase concentration in a non-linear fashion. Therefore it can be assumed that the parameters obtained will provide only a rough description of the true competitive behavior of the two compounds. The results of the calculations are summarized in Table 8.

The retention times for the selected test compounds could be predicted with these isotherms

Table 8
Competitive adsorption isotherm parameters of Chiralpak® AS™ and Chiralpak® AS-V™

Compound	Column No.	λ_1	$N_1 K_1$	K_1	$N_2 K_2$	K_2	\bar{N}_i
Compound A	1	0.7	0.033	0.0037	0.173	0.0192	9
	2	0.7	0.052	0.0021	0.227	0.0094	24
	3	0.7	0.079	0.0026	0.252	0.0084	30
	4	0.7	0.073	0.00073	0.418	0.0041	100
Tröger's base	1	1.0	0.194	0.0176	0.503	0.0457	11
	2	0.9	0.114	0.0126	0.270	0.0300	9
	3	1.0	0.069	0.0098	0.255	0.0364	7
	4	0.9	0.0058	0.563	0.563	0.0255	22
<i>trans</i> -Stilbene oxide	1	1.0	0.844	0.422	1.109	0.5545	2
	2	1.7	0.141	0.047	0.335	0.111	3
	3	1.2	0.068	0.0052	0.179	0.0137	13
	4	1.0	0.375	0.0197	0.734	0.0386	19

surprisingly well, however, some deviations ($\pm 5\%$) were observed. It should be noted that the isotherm parameters do not represent actual thermodynamic adsorption mechanisms, but should be considered as a working hypothesis that has to be refined when there is need for a further elucidation of the adsorption behavior under investigation.

In all cases the isotherms for Chiralpak® AS-V™ (column 4) are the most favorable—as can be seen when comparing the saturation capacity \bar{N}_i for the three separations. Surprisingly, for compound A the calculated saturation capacity is even in the range observed normally only for bulk polymeric chiral phases, such as cellulose triacetate (25–75 g/l) [32]. The calculations imply that for the separation of compound A the material in columns 2 and 3 is almost identical and the material in column 1 is

inferior for this separation. For the separation of Tröger's base columns 1, 2, and 3 can be considered as very similar and no significant differences have to be expected for an up-scaling of that separation. In the case of *trans*-stilbene oxide several differences can be observed. The results for columns 1 and 2 are prohibitive for any attempt to separate significant amounts of the compound. The material in columns 3 and 4, however, would allow satisfactory productivities in the SMB mode.

4.3. Prediction of operating conditions

To find satisfactory and optimal operating conditions for a SMB unit experimentally is very tedious and time consuming. Therefore Novasep provides a

Table 9
Comparison of predicted optimal operating parameters for Chiralpak® AS™ and Chiralpak® AS-V™

Operating parameters	Chiralpak® AS™	Chiralpak® AS-V™
Feed concentration (g/l)	32	32
Recycling flow (Zone 1) (ml/min)	390.00	332.85
Extract flow (ml/min)	51.89	67.44
Feed flow (ml/min)	24.00	45.67
Eluent flow (ml/min)	75.64	86.55
Raffinate flow (ml/min)	48.55	64.78
m_1	1.013	1.184
m_2	0.790	0.809
m_3	0.893	1.063
m_4	0.684	0.702
Expected purity raffinate (%)	99.3	99.86
Expected purity extract (%)	99.07	99.47
Expected productivity (kg/day)	1.10	2.10

software package which allows to model non-linear chromatography using laboratory results as described in section 4.2. Assuming a SMB unit with a configuration of 2-2-2-2 with 8 chromatographic columns (cf. Fig. 1) it is possible to predict starting and operating parameters for a pilot-scale SMB unit. Table 9 shows a comparison of operating parameters and predicted purities and productivities for the optimized separation of compound A on Chiralpak® AS™ and Chiralpak® AS-V™.

Table 9 highlights one of the advantages of the so-called “triangle theory” [4]. The possibility to compare predicted performances on a basis of four dimensionless numbers (cf. Eq. (6)), neglecting parameters like different column volumes, different internal flow-rates and switch times and even differences in enantioselectivity and loading capacity. The proposed flow-rate ratios for the separation of compound A are slightly higher for Chiralpak® AS-V™ due to the higher enantioselectivity in comparison to Chiralpak® AS™ and the favorable isotherm, which allows a higher feed flow-rate without loss in purity in both streams leaving the unit. However, the predicted operating points usually have to be refined in order to compensate for differences in the overall porosity between analytical and preparative columns.

4.4. Analysis of the preparative separation

The racemic compound A was obtained through a multi-step synthesis in kg amounts and was subsequently separated using the Licosep 10×50 unit described in Section 2.5. One of the obtained enantiomers was converted in a further multi-step synthesis into a final drug intended for phase I studies [1]. 1.07 kg racemate were separated [extract: 98.17% enantiomeric excess (ee), raffinate: 99.99% ee] within one day/kg CSP (Chiralpak® AS™). Unfortunately the separations was complicated by an increase in back-pressure in the unit from an original 39 bar to 105 bar, a value which is far beyond the specifications of the unit. After the completion of the separation (~14 kg racemate) the CSP had to be replaced. During that process it was discovered that all frits of the eight columns were blocked by small particles which had a similar composition as the packing material.

In order to understand the impact of replacing

Chiralpak® AS™ with Chiralpak® AS-V™ on the separation the so-called “triangle theory” proved to be very helpful. This theory allows an easy graphical description of the internal flow-rates and the switch time which are determining the flow-rate ratios. The projection of the regions of separation on the m_2, m_3 plane spanned by the flow-rate ratios of the two key sections is drawn in Fig. 7.

Several areas in this plane can be distinguished. A triangular region describes an area where the flow-rates in sections 2 and 3 of the SMB lead to a complete separation. This triangle is determined through the adsorption isotherm and the two points on the diagonal are equivalent to the Henry constants (see below). Above this triangle a region is found where only the extract stream is pure, and on the left side of this triangle a region can be found where only the raffinate stream is pure. Over the vertex of the triangle another region is located, where none of the streams is pure. The area under the diagonal of the m_2, m_3 plane has no physical meaning. The interested reader is referred to the literature where the “triangle theory” is explained and applied in great detail [3–5].

The Henry constants give the slope of the com-

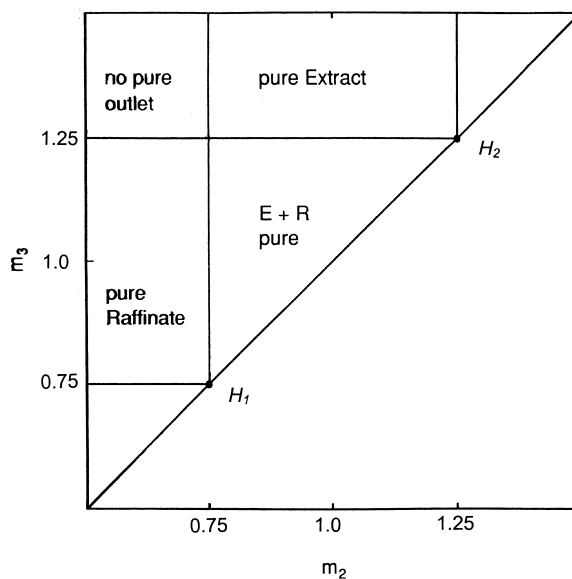


Fig. 7. Regions in the m_2, m_3 plane with different separation regimes in terms of purity of the outlet streams, for a system described by the linear isotherm (cf. Eq. (8)): $H_1 = 0.75$, $H_2 = 1.25$.

Table 10

Henry constants obtained for compound A on analytical and preparative HPLC columns^a

	Analytical columns		Preparative columns	
	H_1	H_2	H_1	H_2
Chiralpak [®] AS [™]	0.77	0.95	0.63	0.85
Chiralpak [®] AS-V [™]	0.77	1.11	0.83	1.22

^a Column dimensions: analytical: 250×0.46 mm I.D.; preparative: 107×48 mm I.D.

ponent's adsorption isotherm under linear conditions, i.e. at infinite concentration:

$$n_i = H_i \cdot c_i \quad (8)$$

At low concentrations the modified Langmuir isotherm (cf. Eq. (7)) allows a calculation of the Henry constants:

$$H_i = N_i K_i + \lambda. \quad (9)$$

The ratio of the Henry constants is equal to the enantioselectivity α . It should be noted that the constants are affected by variations in the bed density (cf. Table 10), respectively the resulting overall porosity ε^* and can be determined from simple experiments [33].

The larger the differences in the Henry constants will be, the larger the triangular region of complete separation (cf. Fig. 7) will become. A comparison of the H_i values in Table 10 shows significant differences between Chiralpak[®] AS[™] and Chiralpak[®] AS-V[™] and indicates that the adsorption isotherms

derived for both CSPs through the pulse experiments described in Section 4.2 might differ for the preparative separation. Chiralpak[®] AS-V[™] should allow for higher feed flow-rates and therefore for a better productivity.

The Novasep software was used to generate a set of starting parameters for the separation of compound A on Chiralpak[®] AS-V[™], which were as follows: Feed concentration = 32 g/l; $Q_{\text{Feed}} = 23.9$ ml/min; $Q_{\text{Eluent}} = 116.0$ ml/min; $Q_{\text{Ex}} = 108.9$ ml/min; $Q_{\text{Ra}} = 31.0$ ml/min; $Q_I = 352.0$ ml/min and column shift period of $t^* = 0.64$ min (cf. Table 11, run A). Interestingly, the operating point proposed by the software was outside the triangular region of complete separation in Fig. 8. Through one linear pulse injection on all eight columns installed in the Licosep 10×50 the arbitrary value for $\varepsilon^* = 0.4$ is corrected through the Novasep software in order to compensate for the different porosity of the stationary phase in the preparative columns. The Licosep 10×50 was started with these parameters and after 10 complete cycles (50 min), the collection of extract and raffinate streams was started. The system was allowed to run for three h and the streams produced were then analyzed. In the raffinate stream no more retained compound could be detected, the extract stream had a purity of $ee = 81.04\%$.

The “triangle theory” suggests that by moving the operating point in a straight line parallel to the diagonal (i.e. without changing Q_{Feed} and Q_{Eluent}) one enters from the region of pure raffinate (run A) either into the triangle of complete separation or the

Table 11

Operating conditions and purities of the outlet streams in the experimental runs of the Licosep 10×50 SMB unit using Chiralpak[®] AS-V[™]

Run No.	Switch time (min)	Flow rates (ml/min)				Flow rate ratios ^a				Experimental ee (%)		Feed concentration (g/l)
		Q_1	Q_2	Q_3	Q_4	m_1	m_2	m_3	m_4	Extract	Raffinate	
A	0.64	352.00	243.10	267.00	236.00	1.281	0.678	0.810	0.639	81.04	100	32
B	0.64	360.00	251.10	275.00	244.00	1.325	0.722	0.855	0.683	95.74	100	32
C	0.64	365.00	256.10	280.00	249.00	1.353	0.750	0.882	0.711	93.09	100	32
D	0.64	360.00	252.10	276.00	236.00	1.325	0.728	0.860	0.639	94.41	100	32
E	0.64	362.20	254.60	278.50	238.50	1.339	0.742	0.874	0.653	98.55	100	32
F	0.64	376.00	264.62	289.29	246.00	1.349	0.751	0.884	0.652	99.31	100	32
G	0.64	376.00	267.62	292.29	246.00	1.349	0.768	0.900	0.652	99.48	100	32
H	0.64	376.00	269.62	294.29	246.00	1.349	0.778	0.910	0.652	99.9	99.9	32
I	0.64	374.19	275.81	300.48	246.19	1.339	0.811	0.944	0.653	99.9	99.9	36

^a For $\varepsilon^* = 0.4$.

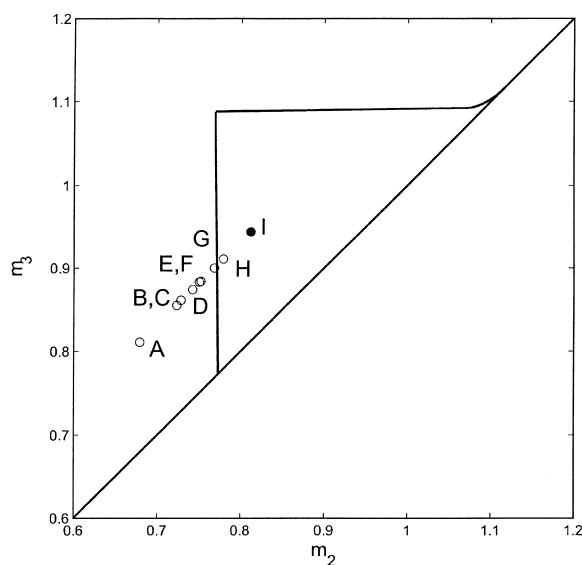


Fig. 8. Separation of compound A in the Licosep 10×50 unit; regions in the m_2 , m_3 plane with different separation regimes in terms of purity of the outlet streams. Predicted region of complete separation: (—) isotherm parameters: $\lambda=0.7$, $H_1=0.77$, $H_2=1.11$, $K_1=0.0007$ l/g, $K_2=0.0041$ l/g, $c_1=c_2=16$ g/l; (○): Operating points corresponding to the runs A to H in Table 11, (●): Operating point corresponding to run I in Table 11.

region of pure extract. This was done in runs B to H (cf. Table 11). As can be seen in Table 11 the purity in the extract stream is increasing steadily the nearer the operating point is to the triangle. The raffinate purity remains unaffected during this increase parallel to the diagonal. The operating point H resulted in complete separation, which is a confirmation of this approach. Therefore it can be assumed that the region of complete separation assumes a similar shape as the predicted triangle. Point I shows the operating point for a higher feed concentration, 36 g/l, close to the solubility limit of the compound. This operating point was used for the separation of 104 kg of racemic compound A. The productivity was 1.45 kg racemate (extract: >99.6% ee, raffinate: >99.9% ee) per day/kg CSP (Chiralpak® AS-V™). No significant problems with an increase in back-pressure or changes in the purity of the product streams were observed. It should be noted that a further improvement of the productivity seems to be possible, but was not attempted in order not to

change the Master Operation Record of the separation which was performed under cGMP guidelines.

5. Conclusion

The physical and chemical properties of the commercial preparative (i.e. 20 μ m particle size) CSP Chiralpak® AS™ and its successor Chiralpak® AS-V™ differ to a considerable degree. The impact of these differences on the SMB separation of a racemic API can be assessed by determining the competitive adsorption isotherms and comparing the predicted optimal operating conditions obtained through software simulation calculations. The calculated operating points can be refined through the recently introduced “method of triangles” which allows to find an optimal operating point for multi-kg separations within one to two days. The new production process for Chiralpak® AS™ seems to have a beneficial effect on enantioselectivity and achievable productivity and has improved the stability of the CSP.

6. Nomenclature

c	mobile phase concentration
H	Henry constant
K	adsorption equilibrium constant
m	flow-rate ratio, defined by Eq. (6)
n	adsorbed phase concentration
\bar{N}	saturation capacity
Q	volumetric flow-rate
Q_s	solid flow-rate in an hypothetical TMB
t^*	switch time in a SMB unit
V	volume of a single column of a SMB
V_S	solid volume in an hypothetical TMB

Greek letters

ε^*	overall void fraction of the bed
λ	linear coefficient of the modified Langmuir isotherm given by Eq. (7)

Subscripts

Eluent	eluent or desorbent
Ex	extract
Feed	feed

<i>i</i>	component index
<i>J</i>	section index
Ra	raffinate
<i>S</i>	solid

Acknowledgements

The authors wish to thank Dr. W. Hauck, Novasep, Vandoeuvre les Nancy, France for his efforts and support during the optimization of the separations, Dr. H.-H. Földner and Dr. K. Pulver, both Solvias, Basel, Switzerland for their help in obtaining the particle distributions and the microscopic images, Dr. G. Cox, Chiral Technologies Europe, Strasbourg, France, for several interesting discussion on the properties of amylose derived CSPs. The helpful advice of Professor M. Mazzotti, Institut für Verfahrenstechnik, ETH Zürich, Switzerland and Professor Dr. M. Morbidelli, Laboratorium für Technische Chemie, ETH Zürich, Switzerland are deeply acknowledged.

References

- [1] M. Juza, M. Mazzotti, M. Morbidelli, *Trends Biotechnol.* 18 (2000) 108.
- [2] M.J. Gattuso, B. McCulloch, J.W. Priegnitz, *Chem. Tech. Europe* 3 (1996) 27.
- [3] M. Mazzotti, M.P. Pedferri, M. Morbidelli, in: *Proceedings of the Chiral Europe '96 Symposium*, 1996, p. 103, Spring Innovations Limited, Stockport, UK.
- [4] M. Mazzotti, G. Storti, M. Morbidelli, *J. Chromatogr. A* 769 (1997) 3.
- [5] A. Gentilini, C. Migliorini, M. Mazzotti, M. Morbidelli, *J. Chromatogr. A* 805 (1998) 37.
- [6] Y. Okamoto, Y. Kaida, *J. Chromatogr. A* 666 (1994) 403.
- [7] E. Yashima, Y. Okamoto, *Bull. Chem. Soc. Jpn.* 68 (1995) 3289.
- [8] L. Miller, C. Orihuela, R. Frontek, D. Honda, O. Dapremont, *J. Chromatogr. A* 849 (1999) 309.
- [9] O. Dapremont et al., WO 99/S7089.
- [10] McCulloch et al., USP 5928515 A.
- [11] G. Hesse, R. Hagel, *Chromatographia* 6 (1973) 277.
- [12] Y. Okamoto, R. Aburatani, K. Hatada, *J. Chromatogr.* 389 (1987) 95.
- [13] Y. Okamoto, M. Kawashima, K. Hatada, *J. Chromatogr.* 363 (1986) 173.
- [14] R.-M. Nicould, *Pharm. Tech. Europe* 11 (3) (1999) 36.
- [15] R.-M. Nicould, *Pharm. Tech. Europe* 11 (4) (1999) 28.
- [16] M. Juza, *J. Chromatogr. A* 865 (1999) 35.
- [17] D. Tondeur, M. Badly, in: R.-M. Nicoud (Ed.), *Simulated Moving Bed—Basics and Applications*, INPL, Nancy, 1993, p. 95.
- [18] Y. Kaida, Y. Okamoto, *Chirality* 4 (1992) 122.
- [19] Y. Okamoto, Y. Kaida, H. Hayashida, K. Hatada, *Chem. Lett.* (1990) 909.
- [20] M. Okamoto, N. Hiroshi, *Biosci., Biotechnol., Biochem.* 56 (1992) 1172.
- [21] R. Kramell, G. Schneider, O. Miersch, *Chromatographia* 45 (1997) 104.
- [22] S. Lin, C.E. Engelsma, N.J. Maddox, B.K. Huckabee, D.M. Sobieray, *J. Liq. Chromatogr. Rel. Technol.* 20 (1997) 1243.
- [23] B.-H. Kim, W. Lee, *Bull. Korean Chem. Soc.* 19 (1998) 289.
- [24] T. Shimizu, M. Enomoto, H. Taka, N. Kamigata, *J. Org. Chem.* 64 (1999) 8242.
- [25] M.S. Villeneuve, R.J. Anderegg, *J. Chromatogr. A* 826 (1998) 217.
- [26] S. Visentin, P. Amiel, A. Gasco, B. Bonnet, C. Suteu, C. Roussel, *Chirality* 11 (1999) 602.
- [27] C. Roussel, C. Suteu, *Enantiomer* 2 (1997) 449.
- [28] C. Roussel, C. Suteu, L. Shaimi, M. Soufiaoui, B. Bonnet, I. Heitmann, P. Piras, *Chirality* 10 (1998) 770.
- [29] *Certificates of Analysis, provided with the CSPs.*
- [30] H.G. Barth (Ed.), *Modern Methods of Particle Size Analysis, Chemical analysis: a series of monographs on analytical chemistry and its applications*, Vol. 73, Wiley, New York, 1984.
- [31] D. Gerlach, *Das Lichtmikroskop*, 1976. Thieme, Stuttgart, Germany.
- [32] J.N. Kinkel, M. Schulte, R.-M. Nicoud, F. Charton, in: *Proceedings of the Chiral Europe '95 Symposium*, 1995, p. 121, Spring Innovations Limited, Stockport, UK.
- [33] E. Francotte, P. Richert, M. Mazzotti, M. Morbidelli, *J. Chromatogr. A* 769 (1998) 239.